第 33 卷第 7 期
2017 年 7 月

无 机 化 学 学 报
CHINESE JOURNAL OF INORGANIC CHEMISTRY

Vol.33 No.7
1139-1146

Co_3O_4/ZnO 修饰针灸针的制备及其在葡萄糖检测领域的应用

苑鸿雯[1] 王玉路[2] 马 驰[3] 耿俊隆[1] 张利强[3] 崔 海*,[1]

([1]首都医科大学中医药学院,中医络病研究北京市重点实验室,北京 100069)

([2]内蒙古科技大学,包头医学院第一附属医院,包头 014010)

([3]中国石油大学(北京)重质油国家重点实验室,北京 102249)

摘要:将 Co_3O_4/ZnO 针状纳米棒材料修饰到针灸针表面用于检测葡萄糖浓度的变化。首先采用水热法在针灸针表面得到 $Co(CO_3)_{0.5}(OH)\cdot 0.11H_2O$ 针状纳米棒前驱体,然后在 500 ℃条件下退火 3 h 得到 Co_3O_4 针状纳米棒阵列。再采用浸渍法将预制备好的 ZnO 量子点修饰到 Co_3O_4 针状纳米棒表面,得到 Co_3O_4/ZnO 复合修饰的针灸针。研究发现此针灸针对葡萄糖具有较好的电流响应(2 264.27 $\mu A\cdot L\cdot mmol^{-1}\cdot cm^{-2}$)、较快的响应速度(<4 s)及较低的检测极限(0.311 $\mu mol\cdot L^{-1}$(*S*/*N*=3))。且该针灸针在用于检测人体模拟细胞液中葡萄糖浓度时,对抗坏血酸和尿素等表现出较强的抗干扰性。

关键词:Co_3O_4; ZnO; 针灸针; 葡萄糖; 传感器

中图分类号:O614.81+2; O614.24+1; R245-33 **文献标识码**:A **文章编号**:1001-4861(2017)07-1139-08

DOI:10.11862/CJIC.2017.118

Co_3O_4/ZnO Modified Acupuncture Needle: Preparation and Application in Detecting Glucose

YUAN Hong-Wen[1] WANG Yu-Lu[2] MA Chi[3] GENG Jun-Long[1] ZHANG Li-Qiang[3] CUI Hai*,[1]

([1]*School of Chinese Medicine, Beijing Key Lab of TCM Collateral Disease Theory Research, Capital Medical University, Beijing* 100069, *China*)

([2]*The First Affiliated Hospital of Baotou Medical College of Inner Mongolia University of Science and Technology, Baotou, Inner Mongolia* 014010, *China*)

([3]*State Key Laboratory of Heavy Oil Processing, China University of Petroleum-Beijing, Beijing* 102249, *China*)

Abstract: A Co_3O_4/ZnO acicular nanorod arrays (ANRAs) decorated acupuncture needle has been fabricated, which demonstrates a good performance for detecting the glucose. Firstly, the precursor $Co(CO_3)_{0.5}(OH)\cdot 0.11H_2O$ ANRAs were fabricated on the acupuncture needle through hydrothermal method. Thereafter, they could be completely converted to the Co_3O_4 ANRAs through annealing at 500 ℃ for 3 h in the air, then ZnO quantum dots (QDs) were decorated on the surface of Co_3O_4 ANRAs through dipping technique. It is found that Co_3O_4/ZnO ANRAs decorated acupuncture needle exhibits a good current response to glucose (2 264.27 $\mu A\cdot L\cdot mmol^{-1}\cdot cm^{-2}$), meanwhile owning a fast response time (<4 s) and a detection limit as low as 0.311 $\mu mol\cdot L^{-1}$ (*S*/*N*=3). Moreover, this acupuncture needle exhibited a high selectivity for glucose in human serum, against ascorbic acid and uric acid.

Keywords: Co_3O_4; ZnO; acupuncture needle; glucose; sensor

收稿日期:2016-12-03。收修改稿日期:2017-04-19。

国家自然科学基金(No.81403467,51401239)资助项目。

*通信联系人。E-mail:drcuihai@163.com

0 Introduction

Acupuncture is good at prophylaxis and treating some certain chronic diseases[1-2]. In the process of acupuncture, acupoints are the main sites of action, which are closely related to the efficacy[3-4]. However, there is no or even negative effect if we needling on the non-acupoints. Exploring the specific differences between the acupoints and non-acupoints is always a hot spot in modern Chinese medicine research[5-6]. According to the metabolomics statistics, it is found that the efficacy of acupuncture has a close relationship with the metabolites changes upon external stimuli, but their specific relationship is not clear, greatly confining evaluating the efficacy of acupuncture[7]. Therefore, quantitatively comparing the biological signals changes on acupoints and non-acupoints upon acupuncture is significant in the study of acupuncture.

A variety of methods have been tried to study biological changes produced upon acupuncture, including positron emission tomography (PET), functional magnetic resonance imaging (fMRI) brain imaging, blood biochemical indices analyze, etc[8-9]. It has been found there exists a significant different brain imaging between acupoints and non-acupoints, and the images from acupoints have a certain physiological specificity[10]. Although the existence of differences between acupoints and non-acupoint has already been confirmed, it stays only in a qualitative level and the specific diversity is still unknown[11]. Moreover, the physiological indictor difference between acupoints and non-acupoints may last only for a short time, which is hard to detect and record. Till now, making an *in situ*, real-time, quantitative detection of the physiological signal changes upon acupuncture is still quite difficult.

In recent years, it is found nano biosensors can detect human metabolism product changes with a fast speed, high efficiency and good accuracy[12-13]. Supposing adding these nano-biosensors during the acupuncture treatment, it may provide a new way for quantitative characterizing biological signals changes on acupoints and non-acupoints upon acupuncture. In all types of biological indicators, charactering the glucose concentration changes is considered as the easiest and most widely used indicator for a clinical practice[13-14]. Various types of glucose biosensor were designed, and wherein the nano-cobalt oxide (Co_3O_4) based biosensors developed rapidly due to its fast response, good anti-interference, wide detection range, and high stability[15-16]. Although various types of nano-Co_3O_4 (nano-films, nanorods, nanotube, *etc.*) based biosensor have been prepared[17-20], no reports have tried fabricating Co_3O_4 acicular nanorod arrays (ANRAs) on the surface of acupuncture needles for making an *in situ*, real-time, quantitative charactering glucose concentration changes. Furthermore, in order to improve the performance of Co_3O_4, ZnO quantum dots (QDs) could be further decorated on the surface of Co_3O_4 ANRAs to form a p-n junction.

Therefore, in this study Co_3O_4/ZnO ANRAs were fabricated on the surface of acupuncture needles by using hydrothermal method. And then, glucose concentration changes were quantitatively monitored through electrochemistry technique by using this acupuncture needle. The Co_3O_4/ZnO decorated acupuncture needle demonstrates a good glucose sensing ability, with a fast response, good anti-interference, wide detection range, and high stability.

1 Experimental

In a typical procedure of fabricating the Co_3O_4 ANRAs, 4 mmol (1.16 g) of cobalt nitrate ($Co(NO_3)_2 \cdot 6H_2O$), 8 mmol (0.29 g) ammonium fluoride (NH_4F) and 8 mmol (1.12 g) of urea ($CO(NH_2)_2$) as sources were dissolved in 40 mL deionized water under stirring at room temperature. After stirring for 20 min, the homogeneous solution was transferred into a 100 mL Teflon lined stainless steel autoclave. An acupuncture needle was immersed in the reaction solution against the bottom of the autoclave. In order to collect enough Co_3O_4 powders for N_2 adsorption-desorption, a piece of cleaned stainless steel foil (80 mm×20 mm) was also immersed in the autoclave. The autoclave was sealed and maintained in an electric

oven at 95 ℃ for 24 h. After cooling down to the room temperature, the acupuncture needle was took out and rinsed with distilled water for several times, and dried at 60 ℃ in vacuum for 2 h. The as-prepared precursors of $Co(CO_3)_{0.5}(OH)\cdot 0.11H_2O$ were converted to Co_3O_4 via thermal decomposition at 500 ℃ in the air for 3 h.

The ZnO QDs were fabricated by dissolving 1.10 g of $Zn(Ac)_2\cdot 2H_2O$ in 50 mL of boiling ethanol. After fully dissolving, the solution was cooled down to 0 ℃, and a white powder was precipitated on the bottom. At the same time, $LiOH\cdot H_2O$ (0.29 g) was dissolved in 50 mL ethanol at room temperature in an ultrasonic bath and the system was cooled to 0 ℃. Then the LiOH solution was added to the Zn $(Ac)_2$ suspension dropwise under vigorous stirring at 0 ℃ until the reaction mixture became transparent. The obtained ZnO QDs solution needs to be stored below 4 ℃ to prevent rapid particle growth. To washing the ZnO solution, ZnO sol and hexane were mixed in the volume ratio of 1∶1. The supernatant was removed by decantation or centrifugation. The ZnO precipitate was re-dispersed in ethanol. This procedure could be repeated several times. After that, ZnO QDs were coated on the Co_3O_4 via a facile soak method.

The structure of sample was characterized by using Bede D1 X-ray diffraction (XRD) system with a Cu $K\alpha$ radiation in the 2θ range of 20°~80° (λ= 0.154 06 nm, U=40 kV, I=40 mA). Surface morphology of all the samples and the element contains were studied by using the FEI Quanta 200F scanning electron microscope (SEM) operated at a voltage of 20 kV equipped with energy-dispersive X-ray spectroscopy (EDX). The X-ray photoelectron spectroscopy (XPS, Thermo Fisher K-Alpha American with an Al $K\alpha$ X-ray source) was used to characterize the Co_3O_4 ANRAs as well. Specific surface areas of the sample was obtained from the results of N_2 adsorption-desorption isotherms at 77 K (Micromeritics ASAP 3020) after using Brunauer-Emmet-Teller (BET) method. The structure of the samples is identified by using the FEI Tecnai G2 F20 transmission electron microscopy (TEM), which is operated at 200 kV. The microscopic Raman spectroscopy was recorded by using a micro-Raman spectrometer (InVia Reflex, Renishaw, UK) with excitation wavelength of 532 nm. All peaks in the Raman spectra were fitted with Lorentzians. All electrochemical measurements, including cyclic voltammetric (CV) and amperometric experiments (I-t) were performed with a CHI 760E electrochemical workstation using the conventional three-electrode system. The Co_3O_4/ZnO decorated acupuncture needle, a platinum sheet, and an Ag/AgCl/KCl electrode were used as the working electrode, counter electrode, and reference electrode, respectively. All electrochemical measurements were conducted in the 1.0 mol·L^{-1} NaOH aqueous solution at room temperature.

2 Results and discussion

As we known, an acupuncture needle can only be used for treating symptoms in the past. However, herein we prepare homogeneous and stable layers of Co_3O_4/ZnO ANRAs on the tip surface of acupuncture needle, adding another significant biosensing function on the traditional acupuncture needle. It is expected that Co_3O_4/ZnO ANRAs modified acupuncture needle can be applied to characterize the biological signals changes through electrochemistry technique, as illustrated in Fig.1.

The fabrication process of Co_3O_4/ZnO ANRAs on the surface of acupuncture needle was schematically

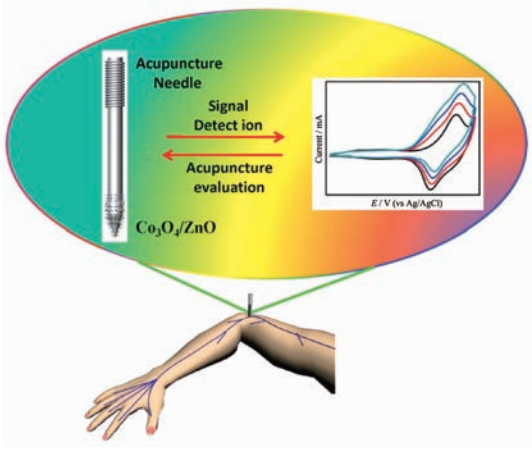

Fig.1 Conceptive illustration of applying Co_3O_4/ZnO modified acupuncture needle for quantitative detecting of the biological index changes upon acupuncture through electrochemistry technique

illustrated in Fig.S1. Firstly, Co related precursor arrays were obtained on acupuncture needle through hydrothermal method by using the $Co(NO_3)_2 \cdot 4H_2O$, NH_4F, and $CO(NH_2)_2$ as sources at 95 ℃ for 24 h. In order to improve the binding force between the Co_3O_4 and acupuncture needles, the surface roughness of acupuncture needle was enhanced prior to the experiment, including sanding with fine sandpaper and then coating with nano gold. After hydrothermal reaction, the surface of the substrate would be covered with pink precursors, which can be fully converted to the black Co_3O_4 via calcination at 500 ℃ for 3 h. And then, ZnO quantum dots (QDs) were decorated on the surface of Co_3O_4 ANRAs through dipping technique. Finally, an acupuncture needle equipped with biosensing function could be obtained by sealing the end of the needle with a little epoxy resin.

The XRD pattern of as-synthesized Co_3O_4/ZnO ANRAs deposited on the surface of acupuncture needle is shown in Fig.2. As the amount of Co_3O_4/ZnO NW on a single needle is not enough for the XRD characterization, we collect the Co_3O_4/ZnO powder from twenty needles. In the XRD pattern of the prepared Co_3O_4, all the diffraction peaks can be indexed to the face-centered cubic Co_3O_4 (PDF#43-1003), which confirms the complete conversion from cobalt carbonate hydroxide to Co_3O_4. As the amount of ZnO is quite small, we did not find any peaks related to ZnO from the XRD pattern. No other impurity was found from the XPS spectrum of the as-prepared Co_3O_4 (Fig.S2). The four obvious vibration bands located at 475, 518, 615 and 686 cm^{-1} in the Raman spectrum also confirmed the good crystal quality of Co_3O_4 ANRAs (Fig.S3)[19].

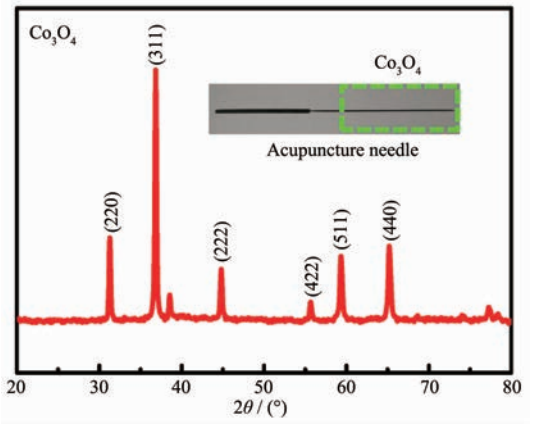

Inset: macroscopic image of the as-prepared sample

Fig.2 XRD pattern of the Co_3O_4/ZnO fabricated on the surface of acupuncture needle

The morphology of the Co_3O_4/ZnO ANRAs was characterized by SEM and TEM (Fig.3). In Fig.3(a), a

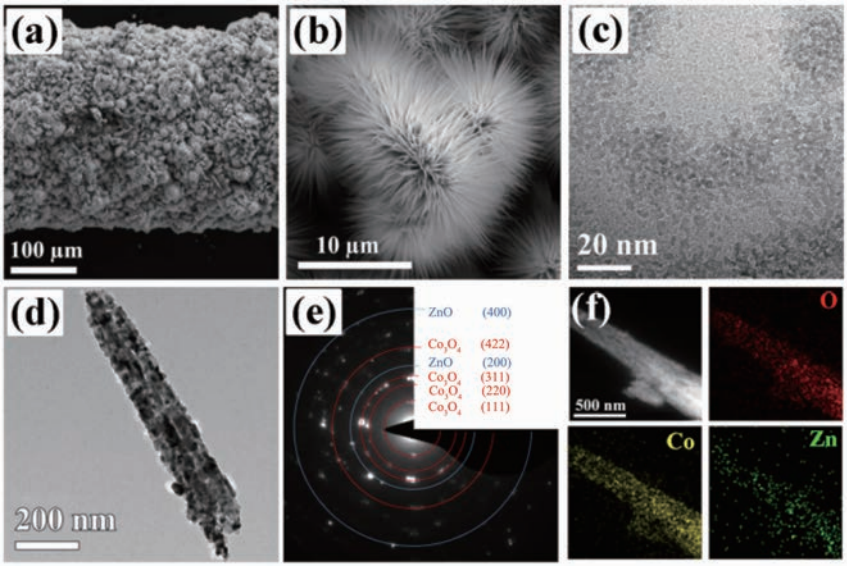

Fig.3 (a) SEM image of the Co_3O_4/ZnO at a low magnification; (b) High magnification SEM image of the pristine Co_3O_4, in which the Co_3O_4 ANRAs are homogeneously aligned on the needle like a cactus ball; (c) TEM image of ZnO QDs at a high magnification; (d) Typical TEM image of Co_3O_4/ZnO in a high magnification; (e) Diffraction pattern of Co_3O_4/ZnO ANRAs; (f) STEM image and related EDX mapping of a single Co_3O_4/ZnO ANRA

large scale and high density Co_3O_4 arrays are found uniformly deposited on the acupuncture needle. From the high magnification SEM image of Co_3O_4 (Fig.3(b)), we found that the Co_3O_4 arrays demonstrate an acicular morphology. Fig.3(c) demonstrates a typical TEM image of the prepared ZnO QDs. The high magnification of Co_3O_4/ZnO is shown in Fig.3(d), from which an obvious acicular like Co_3O_4 ANRAs was observed, and the length of Co_3O_4 ANRAs were ~1 μm. After annealing, plenty of nanopores were formed in the Co_3O_4 ANRAs, which may be generated due to the dehydration and lattice contraction occurring during the thermal treatment. These nanopores existed in the Co_3O_4 lead to a relative large S_{BET} (~20 $m^2 \cdot g^{-1}$) compared to that of the as-prepared precursor (~3 $m^2 \cdot g^{-1}$). From Fig.3(d), it is also found that Co_3O_4 ANRAs are not a single crystal but composed by a lot of nanocrystals, which own a large surface accompanying with plenty of highly active surfaces exposed. Fig.3(e) shows the diffraction pattern of the Co_3O_4/ZnO ANRAs, in which the circles were attributed to Co_3O_4/ZnO. Fig. 3(f) shows the STEM image of the Co_3O_4/ZnO, from which it is found that the ZnO QDs are uniformly decorated on the surface of Co_3O_4.

The electrochemical behaviors of the modified electrode were studied by cyclic voltammetry (CV). Fig.4(a) compares the CV curves of the bare needle, Co_3O_4 decorated needle, and Co_3O_4/ZnO ANRAs modified acupuncture needle in the potential range of −0.1~0.6 V (vs Ag/AgCl) at a scan rate of 40 $mV \cdot s^{-1}$. The experiments were carried out in alkaline solution (1.0 $mol \cdot L^{-1}$ NaOH). It is found that there are not any peaks for the bare needle. While for the Co_3O_4, two pairs of redox peaks appear, which could be further improved after decorated with ZnO. Herein, a typical p-n heterojunction is formed when n-type ZnO is decorated on p-type Co_3O_4, which improves its biosensing response. The electrochemical performance of pure ZnO electrode for detecting glucose is shown in Fig.S4, in which almost no current response can be observed after the addition of glucose. Since ZnO has almost no response to the glucose, we only explore the behavior of Co_3O_4. The first pair of redox peaks appeared at around 0.1 V (Fig.4(a), Inset) can be ascribed to the reversible transition between Co_3O_4 and CoOOH (Reaction 1), and the other redox peak (0.5 V) can be assigned to the conversion of CoOOH and CoO_2 (Reaction 2)[21]. These two reversible reactions can be represented by the following equations:

$$Co_3O_4+OH^-+H_2O \rightleftharpoons 3CoOOH+e^- \quad (1)$$

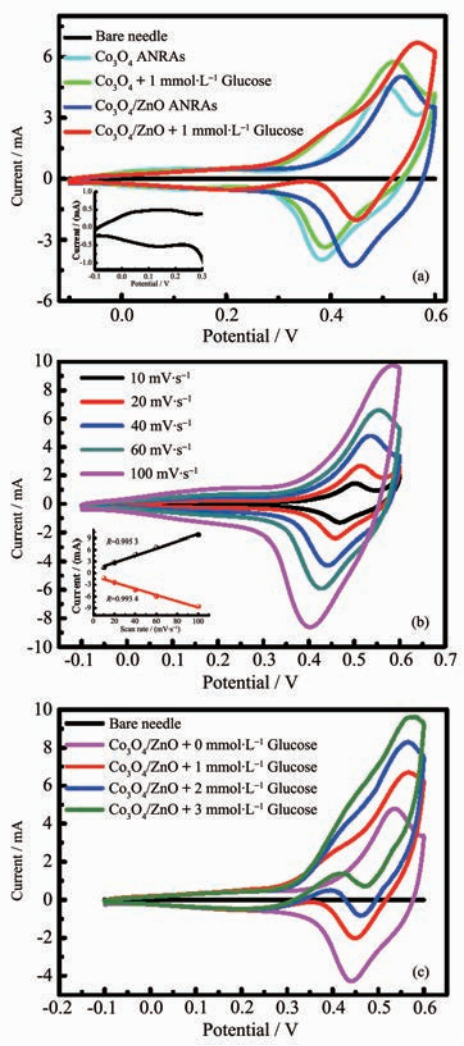

Inset: (a) CV curves of the Co_3O_4 ANRAs electrode in the presence of glucose at a high magnification; (b) Relationship between the redox peak currents and the scan rate in the range from 10 to 100 $mV \cdot s^{-1}$

Fig.4 (a) CV curves of the bare acupuncture needle, Co_3O_4 and Co_3O_4/ZnO ANRAs modified acupuncture needle electrode in the presence and absence of glucose; (b) Co_3O_4/ZnO electrode at different scan rates; (c) CV curves of the Co_3O_4/ZnO ANRAs modified acupuncture needle electrode in the presence of glucose with different concentrations

$CoOOH+OH^- \rightleftharpoons CoO_2+H_2O+e^-$ (**2**)

Upon the injection of glucose (concentration of glucose in alkaline solution is 1 mmol·L^{-1}), the CV curves of Co_3O_4 quickly shift to more positive values especially in the anodic peaks. With the increased scan rate from 10 to 100 mV·s^{-1}, the current density demonstrates an apparent higher response, indicating a surface-controlled process of redox reaction of Co_3O_4 on acupuncture needle (Fig.4(b)). The liner response behavior (Fig.4(b), Inset) manifests that the modified acupuncture needle might be used for quantitative detecting the concentration of glucose in situ. The biosensing mechanism can be roughly summed up through the following equation 3 of the electrochemical oxidation reaction from glucose to gluconolactone catalyzed by Co_3O_4[22]:

$CoO_2+glucose \rightarrow CoOOH+gluconolactone$ (**3**)

As this reaction proceeds, CoO_2 attendant are consumed, contributed to the occurrence of the positive reaction of equation 2, which synchronously leads the current density increases and results in the detection of the addition of glucose (Fig.4(c)).

Fig.5(a) displays the amperometric responses of Co_3O_4 and Co_3O_4/ZnO ANRAs electrode to successive addition of glucose with serial concentrations. The suitable sensing potential is determined to be 0.55 V from the CV curves, and a current density-time plot was obtained by the successive addition of different concentration of glucose solution into 1.0 mol·L^{-1} NaOH solution. The initial rate for the addition of glucose is 0.2 mmol·L^{-1} till the total glucose concentration in alkaline solution reached 1 mmol·L^{-1}, during which the glucose increment was made at the rate of 0.2 mmol·L^{-1}, and each rate dropped five times with an interval of 50 s till the end. The starting points of additions of glucose at different rate are noted by black arrows in Fig.5 (a). It is found that Co_3O_4/ZnO ANRAs demonstrate a higher response to

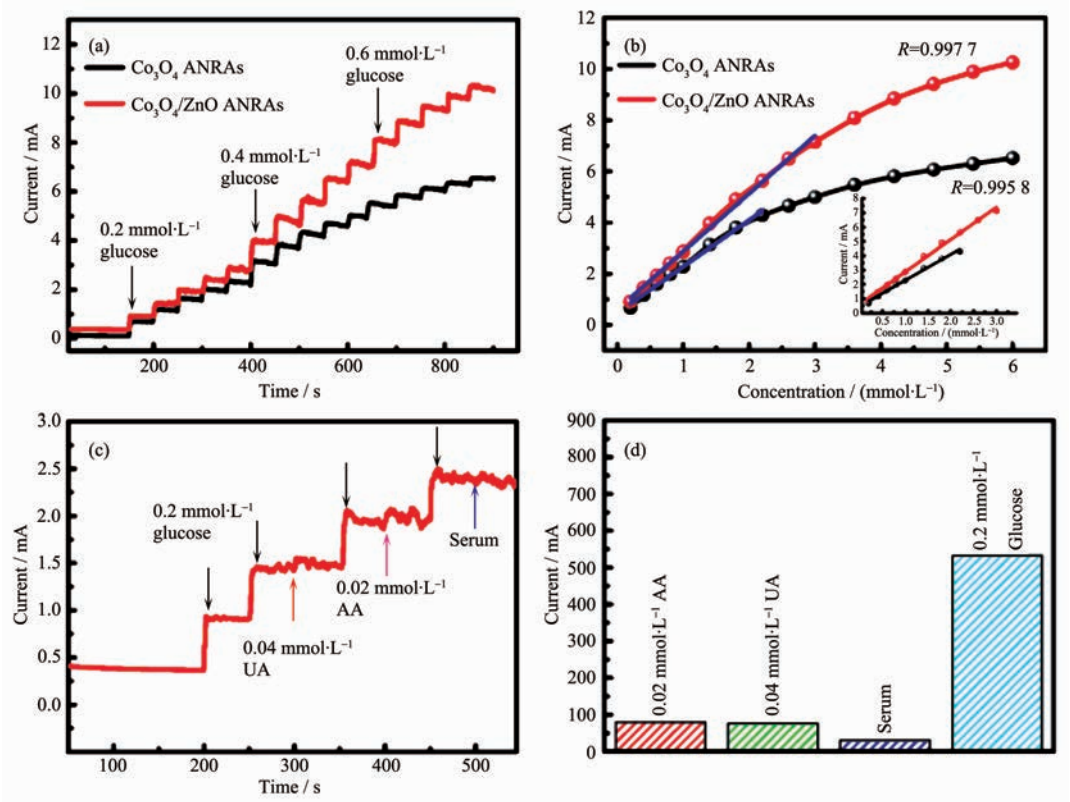

Fig.5 (a) Amperometric response to successive addition of glucose obtained by using Co_3O_4/ZnO electrode at an applied potential of 0.55 V; (b) Corresponding calibration curves from (a); (c) Amperometric response of Co_3O_4/ZnO electrode to successive addition of 0.2 mmol·L^{-1} glucose with intervals of 100 s, and 0.02 mmol·L^{-1} AA, serum and 0.04 mmol·L^{-1} UA were respectively injected to the NaOH solution (1.0 mol·L^{-1}) in the middle of each interval; (d) Current density response columnar diagram of the tested analytes compared with glucose

the addition of glucose than Co_3O_4. To further study the amperometric performance of Co_3O_4/ZnO ANRAs electrode, a calibration curve for glucose is constructed by evaluating the fluctuation in current density with each addition of glucose solution at a certain concentration shown in Fig.5(b). The linear range of Co_3O_4/ZnO electrode′s glucose sensing is 0.2~3.0 mmol·L^{-1} (R=0.997 7), and the linear relationship between the response current and the glucose concentration is given by the equation y=2 264.27x+602.53 (x is the glucose concentration (mmol·L^{-1}), y is the response current (μA)). Besides, from the slope of the two fitted curves, the sensitivity of Co_3O_4/ZnO electrode was determined to be 2 264.27 μA·L·mmol^{-1}·cm^{-2}. A rapid response time (<4 s) and a remarkable low detection limit of 0.311 μmol·L^{-1} (S/N=3) are also interpreted from Fig.5(b), which are also better than those of the pristine Co_3O_4.

The selectivity of the Co_3O_4/ZnO ANRAs was investigated against ascorbic acid (AA), serum and uric acid (UA). The amperometric detection was conducted at the potential of 0.55 V in 1 mol·L^{-1} NaOH solution under stirring. After the current density of the curve leveled off, 0.2 mmol·L^{-1} (glucose concentration in total NaOH solution) glucose was continuous added to the NaOH solution at intervals of 100 seconds. In the middle of the interval, 0.02 mmol·L^{-1} AA, pure serum, 0.04 mmol·L^{-1} UA were successive injected to the NaOH solution. As shown in Fig.5(c), stepped curve remained intact form after the addition of interferent, which indicates that AA, pure serum and UA will not prevent the selective detection of glucose. What is noteworthy is that there are a large number of different categories of proteins and biomolecules in the serum, the Co_3O_4 electrode can still keep its highly resistant to interference. The current density response columnar diagram of each kind of interferent compared with glucose is demonstrated clearly in Fig.5(d), which confirms the highly anti-interference ability of Co_3O_4/ZnO ANRAs electrode. A comparison of the Co_3O_4/ZnO ANRAs composite with some of the reported non-enzymatic glucose biosensors based on metal oxides or metal hydroxides is summarized in Table 1[16-17,20,23-28]. It is found that the Co_3O_4/ZnO ANRAs exhibit satisfactory performances including high sensitivity, low detection limit and wide linear range. In particular, it has obviously higher sensitivity and lower detection limit than those reported previously.

Additionally, we tried to use this acupuncture needle to characterize the glucose with unknown concentration in an assumed solution. Through measuring the current (2.4 mA), it is calculated the concentration of glucose is 1.07 mmol·L^{-1}, which is in a relatively agreement with the presetting concentration (1 mmol·L^{-1}). Additionally, the concentration of glucose was *in situ* changed by adding more glucose into the solution or dissolving it with more water. In this process, the current occurred a rapid response, proving that this acupuncture needle might make an

Table 1　Comparison of as-prepared sensors with other reported glucose biosensors in performance

Sample	Linear range / (mmol·L^{-1})	Sensitivity / (μA·L·mmol^{-1}·cm^{-2})	Detection limit / (μmol·L^{-1})	Applied potential / V	Response time / s	Reference
Co_3O_4/ZnO ANRAs	Up to 3.0	2 264.27	0.311	+0.55	<4	This work
Co_3O_4/Graphene	0.05~0.3	—	10	+0.55	—	[23]
Co_3O_4 microspheres	0.002~1.48	68.77	—	+0.55	5	[24]
CuO_x-CoO_x/rGO	0.005~0.57	42.03	0.5	+0.5	3	[25]
Co_3O_4/3D Graphene	Up to 0.08	122.16	0.157	+0.58	<7	[26]
Co_3O_4/PbO_2	0.005~1.2	460.3	0.31	+0.55	<3	[27]
Co_3O_4 nanowires	0.000 1~12	45.8	0.026	+0.5	—	[16]
Co_3O_4/MPC	0.1~0.9	1 145.2	10	+0.55	3	[20]
Co_3O_4 ANTA	0.01~2.1	1 765.90	0.339 6	+0.5	<5	[17]
$NiCo_2O_4$/3D GF	0.000 5~0.59	818.51	0.38	+0.5	<10	[28]

in situ, real-time, quantitative charactering the glucose concentration changes.

3 Conclusions

In summary, a novel acupuncture needle with biosensing function was fabricated by coating with Co_3O_4/ZnO ANRAs on its surface through a hydrothermal method. The structure and morphology of Co_3O_4/ZnO were characterized by XRD, SEM, and TEM, which confirmed that Co_3O_4/ZnO ANRAs were uniformly distributed on the surface of acupuncture needle. This bio-functional acupuncture needle demonstrates excellent sensitivity, fast amperometric response, low detection limit and good selectivity for the detecting of glucose. The large specific surface area provided by Co_3O_4/ZnO ANRAs and the good sensing abilities of Co_3O_4 contribute to its excellent performance. The success of adding the biosensing function on the acupuncture needle provide a novel way to *in situ* monitoring biological indicator concentration changes upon acupuncture, which is significant for quantitative evaluating and understanding the clinical efficacy of acupuncture in modern Chinese medicine.

Acknowledgments: YUAN Hong-Wen and WANG Yu-Lu contribute equally to this work. This work is financially supported by the National Natural Science Foundation of China (Grants No.81403467, 51401239).

Supporting information is available at http://www.wjhxxb.cn

References:

[1] Raith W, Li Y, Zheng H, et al. *Dtsch. Z. Akupunktur*, **2012**, **55**(4):22-24

[2] Napadow V, Ahn A, Longhurst J, et al. *J. Altern. Complement Med.*, **2008**,**14**(7):861-869

[3] Kaptchuk T J. *Ann. Int. Med.*, **2002**,**136**(5):374-383

[4] Leake R, Broderick J E. *Integr. Med.*, **1999**,**1**(3):107-115

[5] Liu C Z, Xie J P, Wang L P, et al. *Pain Med.*, **2014**,**15**(6):910-920

[6] Ma T T, Yu S Y, Li Y, et al. *Aliment. Pharmacol. Ther.*, **2012**,**35**(5):552-561

[7] Fuentealba Cargill F, Biagini Alarcón L. *Rev. Med. Chile*, **2016**,**144**(3):325-332

[8] Zhao Z Q. *Prog. Neurobiol.*, **2008**,**85**(4):355-375

[9] Mayer D J. *Progress in Brain Research. Vol.*122. Mayer E A, Saper C B Ed., Amsterdam: Elsevier, **2000**:457-477

[10]Li L, Liu H, Li Y Z, et al. *J. Altern. Complement Med.*, **2008**,**14**(6):673-678

[11]Garcia M K, McQuade J, Haddad R, et al. *J. Clin. Oncol.*, **2013**,**31**(7):952-960

[12]Anker J N, Hall W P, Lyandres O, et al. *Nat. Mater.*, **2008**, **7**(6):442-453

[13]Tian K, Prestgard M, Tiwari A. *Mater. Sci. Eng. C*, **2014**,**41**: 100-118

[14]Scognamiglio V. *Biosens. Bioelectron.*, **2013**,**47**:12-25

[15]Ding Y, Wang Y, Su L, et al. *Biosens. Bioelectron.*, **2010**,**26** (2):542-548

[16]Khun K, Ibupoto Z H, Liu X, et al. *Mater. Sci. Eng. B*, **2015**, **194**:94-100

[17]Gao Z, Zhang L, Ma C, et al. *Biosens. Bioelectron.*, **2016**, **80**:511-518

[18]Fan S, Zhao M, Ding L, et al. *J. Electroanal. Chem.*, **2016**, **775**:52-57

[19]Zhang L, Gao Z, Liu C, et al. *J. Mater. Chem. A*, **2015**,**3**(6): 2794-801

[20]Li M, Han C, Zhang Y, et al. *Anal. Chim. Acta*, **2015**,**861**: 25-35

[21]Casella I G, Gatta M. *J. Electroanal. Chem.*, **2002**,**534**(1):31 -38

[22]Heli H, Yadegari H. *Electrochim. Acta*, **2010**,**55** (6):2139-2148

[23]Wang X, Dong X, Wen Y, et al. *Chem. Commun.*, **2012**,**48** (52):6490-6492

[24]Yin H, He X, Cui Z, et al. *IET Micro Nano Lett.*, **2016**,**11** (3):151-155

[25]Li S J, Hou L L, Yuan B Q, et al. *Microchim. Acta*, **2016**,**183** (6):1813-1821

[26]Bao L, Li T, Chen S, et al. *Small*, **2017**,**13**(5):DOI:10.1002/ smll.201602077

[27]Chen T, Li X, Qiu C, et al. *Biosens. Bioelectron.*, **2014**,**53**: 200-206

[28]Wu M Y, Meng S J, Wang Q, et al. *ACS Appl. Mater. Interfaces*, **2015**,**7**(38):21089-21094